Published in final edited form as:
J Cell Physiol. 2015 October ; 230(10): 2447–2460. doi:10.1002/jcp.24975.

A SMYD3 Small-Molecule Inhibitor Impairing Cancer Cell Growth

Alessia Peserico[#1,2], **Aldo Germani**[#1], **Paola Sanese**[#1], **Armenio Jorge Barbosa**[3], **Valeria Di Virgilio**[1], **Raffaella Fittipaldi**[4], **Edoardo Fabini**[5], **Carlo Bertucci**[5], **Greta Varchi**[6], **Mary Pat Moyer**[7], **Giuseppina Caretti**[4], **Alberto Del Rio**[3,6,*], and **Cristiano Simone**[1,2,**]

[1]Division of Medical Genetics, Department of Biomedical Sciences and Human Oncology (DIMO), University of Bari “Aldo Moro”, Bari, Italy

[2]National Cancer Institute, IRCCS Oncologico Giovanni Paolo II, Bari, Italy

[3]Department of Experimental, Diagnostic and Specialty Medicine (DIMES), Alma Mater Studiorum University of Bologna, Bologna, Italy

[4]Department of Biosciences, University of Milan, Milan, Italy

[5]Dipartimento di Farmacia e Biotecnologie, University of Bologna, Bologna, Italy

[6]Institute of Organic Synthesis and Photoreactivity (ISOF), National Research Council (CNR), Bologna, Italy

[7]INCELL Corporation, San Antonio, Texas

[#] These authors contributed equally to this work.

Abstract

SMYD3 is a histone lysine methyltransferase that plays an important role in transcriptional activation as a member of an RNA polymerase complex, and its oncogenic role has been described in different cancer types. We studied the expression and activity of SMYD3 in a preclinical model of colorectal cancer (CRC) and found that it is strongly upregulated throughout tumorigenesis both at the mRNA and protein level. Our results also showed that RNAi-mediated SMYD3 ablation impairs CRC cell proliferation indicating that SMYD3 is required for proper cancer cell growth. These data, together with the importance of lysine methyltransferases as a target for drug discovery, prompted us to carry out a virtual screening to identify new SMYD3 inhibitors by testing several candidate small molecules. Here we report that one of these compounds (BCI-121) induces a significant reduction in SMYD3 activity both in vitro and in CRC cells, as suggested by the analysis of global H3K4me2/3 and H4K5me levels. Of note, the extent of cell growth inhibition by BCI-121 was similar to that observed upon SMYD3 genetic ablation. Most of the results described above were obtained in CRC; however, when we extended our observations to tumor cell lines of different origin, we found that SMYD3 inhibitors are also effective in other cancer types, such as lung, pancreatic, prostate, and ovarian. These results represent the proof of

[*]Correspondence to: Alberto Del Rio, Department of Experimental, Diagnostic and Specialty Medicine (DIMES), Alma Mater Studiorum University of Bologna, Bologna, Italy. alberto.delrio@gmail.com. [**]Correspondence to: Cristiano Simone, Division of Medical Genetics, Department of Biomedical Sciences and Human Oncology (DIMO), University of Bari “Aldo Moro”, Bari, Italy. cristianosimone73@gmail.com.

Conflict of interest: The authors have no conflict of interest to declare.

Europe PMC Funders Author Manuscripts

principle that SMYD3 is a druggable target and suggest that new compounds capable of inhibiting its activity may prove useful as novel therapeutic agents in cancer treatment.

Cancer cell fate is governed by an intricate network of signaling pathways that intersect with epigenetic regulators at the chromatin level. Indeed, any altered signaling cascade can induce a perturbation of chromatin structure and functions resulting in modulation of gene expression (Suganuma and Workman 2012; Klein et al., 2013). One prominent mechanism regulating chromatin dynamics is the post-translational modification of histone proteins. Histone methylation is an important and widespread type of chromatin modification that is known to affect biological processes involved in several types of cancer. Moreover, changes in global histone methylation patterns were observed in cancer development together with deregulation of the enzymes responsible for adding and removing methyl marks (Copeland et al., 2009; Chi et al., 2010; Varier and Timmers, 2011; Greer and Shi, 2012).

The histone methyltransferase SET/MYND Domain Type of Zinc Finger (SMYD3), a member of the subfamily of SET domain-containing proteins (Foreman et al., 2011), has been found overexpressed in different types of tumors: breast, gastric, pancreatic, colorectal, lung cancer, and hepatocellular carcinoma (Tsuge et al., 2005; Hamamoto et al., 2004, 2006; Liu et al., 2014; Mazur et al., 2014). In normal cells, SMYD3 seems to be dispensable for development, as well as for proliferation and survival. Indeed, SMYD3 homozygous conditional KO mice, both male and female, did not show any significant abnormality after full phenotyping (www.sanger.ac.uk/mouseportal/search?query=smyd3). However, SMYD3 overexpression in normal cells is sufficient to accelerate cell growth and has a key role in the activation of genes downstream of pathways involved in tumor cell transformation and migration (Cock-Rada et al., 2012; Luo et al., 2014).

Despite the link existing between SMYD3 deregulation and tumorigenesis, the mechanisms underlying SMYD3 modulation and its ability to promote uncontrolled cancer cell proliferation have not been fully elucidated yet. Silencing of SMYD3 has been reported to significantly impair cell proliferation in CRC, hepatocellular carcinoma, fibrosarcoma, and breast cancer cells (Hamamoto et al., 2004, 2006; Cock-Rada et al., 2012; Guil et al., 2012). These preliminary observations suggest the involvement of SMYD3 in cell cycle deregulation, one of the critical steps in the development of cancer.

Several studies have been designed to explore the oncogenic activity of SMYD3. Initially, SMYD3 was described as a histone H3K4-specific di- and tri-methyltransferase eliciting its oncogenic effect through transcriptional activation of its downstream target genes [e.g., WNT10B, NKX2.8, CDK2, cMET, TERT] (Hamamoto et al., 2004, 2006; Liu et al., 2007; Zou et al., 2009); however, recent studies identified histone H4 as a preferred substrate in in vitro binding assays. Besides, it has been shown that SMYD3 is required for H4K5 methylation in culture and that its enzymatic activity is important for maintaining the transformed cellular phenotype associated with high SMYD3 expression (Van Aller et al., 2012).

SMYD3 oncogenic activity may also involve functional interactions with non-histone proteins (e.g., VEGFR1, estrogen receptor [ER]) in the cytoplasm that regulate cancer cell

Europe PMC Funders Author Manuscripts

proliferation and survival. Indeed, SMYD3 methylates VEGFR1, thereby enhancing its kinase activity in cancer cells, and acts as a coactivator of ER in breast cancer cells (Kunizaki et al., 2007; Kim et al., 2009; Biggar and Li 2014). Furthermore, mutated KRAS correlates with SMYD3 upregulation in CRC, and methylation of MAP3K2 by SMYD3 increases MAP kinase signaling, thereby promoting the development of lung and pancreatic cancer (Gaedcke et al., 2010; Mazur et al., 2014).

Here we show that SMYD3 expression increases during carcinogenesis, along with its downstream targets. We also found that SMYD3 is overactivated in a number of cancer cell lines, with cells expressing high levels of SMYD3 being highly sensitive to its genetic depletion. Besides, by means of molecular docking techniques we identified a small-molecule compound (BCI-121) which significantly inhibits SMYD3-substrate interaction and chromatin recruitment and is effective in reducing proliferation in various cancer cells types.

Materials and Methods

Cell culture and reagents

HT29, Caco-2, SW480, LoVo, LS174T, HCT116, A549, MDA-MB-468, Hep3b, OVCAR-3, SKOV-3, and DU145 (all from ATCC LGC, Sesto San Giovanni, MI) cell lines were grown in DMEM supplemented with 10% FBS (HT29, SW480, LS174T, A549, MDA-MB-468, Hep3b, OVCAR-3 SKOV-3, DU145, and HCT116) or 20% FBS (Caco-2 and LoVo). DLD-1 and Capan-1 (from ATCC) cell lines were grown in RPMI-1640 supplemented with 10% FBS. The NCM460 cell line was received under a material transfer agreement with INCELL Corporation. These cells were routinely propagated under standard conditions in M3:10 medium (INCELL). All media were prepared with 100 IU/ml penicillin and 100 μg/ml streptomycin, cells were grown in a humidified incubator at 37 °C and 5% CO_2 avoiding confluence at any time. For RNAi, cells were transfected with 5 nM Stealth siRNA directed against SMYD3 by using HiPerFect Transfection Reagent (Qiagen) according to the manufacturer's instructions. On-TARGET-plus control siRNA (Thermo Scientific) was used as a control sequence (siRNA sequences are available upon request). All screened compounds were dissolved in dimethyl sulfoxide (DMSO) and stored at –20 °C. The tested BCI-121 concentration is indicated in figure legends.

In vivo studies

Normal, adenoma, and adenocarcinoma colon mucosa tissues were obtained from $APC^{Min/+}$ control mice (n = 10) and $APC^{Min/+}$ mice treated with 12 mg/kg of azoxymethane (AOM) (Sigma) (n = 10). Procedures involving $APC^{Min/+}$ mice were previously described (Chiacchiera et al., 2009). Experiments involving animals and their care were conducted in conformity with the institutional guidelines that are in compliance with national and international laws and policies.

Quantitative real-time PCR

Total RNA was extracted using TRI reagent (Sigma) according to the manufacturer's instructions. Samples were retro-transcribed using the High Capacity DNA Archive Kit

Europe PMC Funders Author Manuscripts

(Applied Biosystem). PCRs were carried out in triplicate using the SYBR Green PCR Master Mix (Bio-Rad) on a CFX96 Touch Real-Time PCR Detection System (Bio-Rad), according to the manufacturer's instructions. Relative quantification was done using the ddCT method. Primer sequences are available on request.

Cell extracts and immunoblot analysis

Whole cell extracts were obtained from cells collected and homogenized in lysis buffer (50 mM Tris-HCl pH 7.4; 5 mM EDTA; 250 mM NaCl; and 1% Triton X-100) supplemented with protease and phosphatase inhibitors (Roche). Nuclear enriched fractions were obtained by using the EpiSeeker Nuclear Extraction Kit (Abcam) according to the manufacturer's instructions. Immunoblots were carried out as previously described (Chiacchiera et al., 2009). 20 μg of protein extracts from each sample were denatured in Laemmli Sample buffer before SDS-PAGE and used for immunoblot analysis. Anti-βActin (Sigma), anti-SMYD3, anti-phospho-p44/42 MAPK (Thr202/Tyr204), anti-p44/42 MAPK, anti-cMyc, anti-Lamin A/C, anti-Histone H3K4me2 (all from Cell Signaling Technology), anti-βTubulin (Santa Cruz Biotechnology), anti-Histone H3K4me3, anti-Histone H3K27me3, anti-Histone H3 (all from Abcam), anti-Histone H4K5me (produced in our Lab) were used as primary antibodies. HRPO-conjugated antibodies (GE Healthcare) were used as secondary antibodies and revealed using the ECL-plus chemiluminescence reagent (GE Healthcare). Densitometric evaluation was performed by ImageJ software.

Cell counting and cell proliferation assays (WST-1)

Cells were counted with a hemocytometer and scored as the number of proliferating cells at different time points (24, 48, 72, and 96 h) for each treatment group. Cell proliferation was also determined using the Cell Proliferation Reagent WST-1 (Roche) according to the manufacturer's instructions. Briefly, cells were seeded into 96-well plates one day before treatment. After 48 h, 72 h, or 96 h of BCI-121 or DMSO exposure, 10 μl of the Cell Proliferation Reagent WST-1 were added to each well and incubated at 37 °C in a humidified incubator for up to 1 h. Absorbance was measured on a microplate reader (BioTek) at 450/655 nm. The proliferation index was calculated as the ratio of WST-1 absorbance of treated cells to WST-1 absorbance of control cells.

Cell synchronization and BrdU incorporation assay

Cells were synchronized by the double thymidine block method (O'Connor and Jackman, 1998). Briefly, cells were incubated in medium containing 2 mM thymidine (Sigma) for 12 h, released into their normal medium for 8–10 h and then incubated for 12 h in medium containing 2 mM thymidine. Cells were seeded on glass coverslips and treated with BCI-121 and/or DMSO 5 h before the first thymidine block and at each thymidine release. The BrdU incorporation assay was performed with the Cell Proliferation Kit (GE Healthcare) according to the manufacturer's instruction. Briefly, BrdU was added at each time point (4 h and 8 h after thymidine release) and cells were incubated for 2 h at 37 °C with 5% CO2. BrdU positive cells were stained with a primary anti-BrdU antibody and then with a secondary fluorescent antibody (Alexa Fluor – Life Technologies). Cells were observed with a Zeiss LSM-5 Pascal microscope and counting was based on 15 randomly chosen fields per

coverslip. Data presented in the “Results” section were obtained by scoring the percentage of BrdU-positive cells.

FACS analysis

Cells were collected, ethanol-fixed and stained with propidium iodide (Sigma). Cell cycle distribution was measured with a FACS Vantage flow cytometer and analyzed using the Cell Quest-PRO software (BD Bioscience).

Chromatin immunoprecipitation (ChIP)

ChIP assays were performed using the MAGnify Chromatin Immunoprecipitation System (Life Technologies) according to the manufacturer’s instructions. IgG antibodies were included in the kit and 1 μg of anti-SMYD3 antibody (Abcam) was used for each assay. PCR was performed on “input” DNA of different samples and equivalent amounts of immunoprecipitated DNA were amplified by real-time PCR as described in the “Quantitative real-time PCR” method section. Quantification was done using the Input % method. The set of primers used for ChIP allows the amplification of target promoter regions including SMYD3 binding sites (sequences are available upon request).

In silico screening and modeling

With the aim of identifying new small-molecule inhibitors targeting the human SMYD3 catalytic site, the Glide (version 5.7) docking software was used to perform a high-throughput virtual screening of the CoCoCo databases (Del Rio et al., 2010). A total of around 260.000 molecules were screened by centering a 20 Å docking grid in the histone binding site of the crystallographic structure (PDB ID). Docking results were ranked based on the Glide score by using the default settings (SP score) and the first 500 hit compounds were visually inspected taking into account several structural and physicochemical rules, such as qualitative evaluation of ligand–protein interactions within the active site, probability of suggested protonation and tautomeric states, stereochemistry complexity, compound availability, and chemical diversity. Based on these criteria, 15 molecules (Table S1) were purchased for experimental testing.

In vitro methylation assay

GST-SMYD3 (Epicypher, Tebu-bio) was incubated with 100 μM BCI-121 or BCI-121 dilution buffer for 30 min at room temperature, and then histones (Roche) and SAM-^{3}H (Perkin Elmer) were added for 45 min at 30 °C. Methylation reactions were performed in 50 mM Tris-HCl (pH 8.0), 10% glycerol, 20 mM KCl, 5 mM MgCl2, 0.02% Triton, and 1 mM PMSF. The reaction mixture was resolved by SDS-PAGE, followed by Coomassie stain and autoradiography.

Surface plasmon resonance (SPR)

Measurements were performed with a Biacore X100 optical biosensor (Uppsala, Sweden), thermostated at 25 °C. Evaluation of sensorgrams and data analysis was performed using the BiacoreTMX100 2.0.1 software. SMYD3 immobilization was obtained through affinity capture. The two flow cells were loaded independently with an anti-GST antibody using the

amine coupling kit from BIAcore according to the standard procedure. The CM5 sensor chip was equilibrated at 25 °C and the system was primed three times using running buffer. A mixture of 1-ethyl-3-(3-dimethylaminopropyl)-carbodiimide hydrochloride (EDC) 0.4 M and N-hydroxysuccinimide (NHS). 0.1 M was freshly prepared and injected at 5 μl/min for 7 min. The anti-GST antibody was diluted at 30 μg/ml in sodium acetate pH 5.0 and injected at 5 μl/min for 180 sec, resulting in approximately 3,000 RUs for each flow cell. Injecting ethanolamine at 5 μl/min for 7 min deactivated the remaining active esters. The active flow cell was loaded with the SMYD3-GST fused protein solution, 2 μg/ml, until reaching approximately 300 RUs and the reference cell was loaded with an equimolar recombinant GST protein to reach approximately 150 RUs. The H4 peptide stock solution was prepared at 128.66 μM and serial dilutions at 64.82 μM, 32.41 μM, 16.21 μM, 1.47 μM were injected at 30 μl/min for 60 sec over the surface and then the complex was allowed to dissociate for 720 sec until reaching a level ± 2.0 RUs relative to the baseline. The affinity Kd of the H4 peptide was derived from kinetic parameters (association and dissociation rate constants, k_{on} and k_{off}). Inhibition of H4 binding to SMYD3 by BCI-121 was obtained by dissolving the compound in running buffer and mixing it with the histone peptide at 1:1 and 2.5:1 ratios. The final concentrations were 72.03 μM for the histone peptide and 72.03 and 183.33 μM for the BCI-121 compound. The resulting solutions were injected at 30 μl/min and association was monitored for 100 sec, after which the running buffer was flowed and dissociation was monitored for 900 sec. Measurements were performed in duplicate and averaged; final results were obtained by subtracting the unspecific binding given by the reference flow cell and normalizing to the baseline injection.

Statistical analysis

The statistical significance of the results was analyzed using the Student's *t*-tail test, and $*P < 0.05$, $**P < 0.01$, and $***P < 0.001$ were considered statistically significant.

Results

SMYD3 is upregulated in in vivo models of tumorigenesis

SMYD3 has been found to be overexpressed in different types of cancer, including those arising in the colon-rectum (Hamamoto et al., 2004, 2006; Tsuge et al., 2005; Liu et al., 2014; Mazur et al., 2014). This prompted us to assess its expression and activity during tumorigenesis by studying $APC^{Min/+}$ mice, a widely used model of cancer development and progression. These mice are heterozygous for a nonsense mutation in the APC gene and develop multiple tumors throughout the intestinal tract. To enhance the adenoma-to-carcinoma transition, mice were also treated with azoxymethane (AOM) (De Robertis et al., 2011). Our results show that SMYD3 was strongly upregulated during tumorigenesis, particularly in the colorectal tract (Fig. 1A). Colorectal adenomas and carcinomas displayed high SMYD3 protein overexpression along with increased H4K5 methylation and H3K4 di-methylation (Fig. 1B). Moreover, gene expression analysis revealed that SMYD3 target genes (cMET, TERT, WNT10B, CDK2) were also upregulated in these tissues (Fig. 1C).

SMYD3 expression is enhanced in cellular models of CRC

Analysis of SMYD3 expression levels in human cell lines showed that SMYD3 was poorly expressed in normal colonocytes (NCM460) (both at the mRNA and protein level), while it was significantly overexpressed in HT29 and HCT116 CRC cells (both at the mRNA and protein level) (Fig. 2A and B). Consistently, mRNA levels of SMYD3 target genes were found to be upregulated (Fig. 2B). Moreover, SMYD3 was overexpressed in three other CRC cell lines (SW480, Caco-2, LoVo), while it was expressed at low levels in LS174T and DLD-1 cells (Fig. 2C). SMYD3 protein levels correlated with the expression of its target genes in all analyzed cell lines (Fig. 2D).

Genetic depletion of SMYD3 affects CRC proliferation

We then used two of these cell lines (HT29 and HCT116) as cellular models to ascertain whether RNAi-mediated SMYD3 ablation could impair CRC cell proliferation. Our results showed that SMYD3 is required for proper cancer cell growth (Fig. 3A and D), as well as for the expression of its target genes (Fig. 3C and F). Moreover, SMYD3 genetic ablation correlated with reduced MEK-ERK signaling and with decreased global levels of histone H3K4me2 and H4K5me methylation. Importantly, a non-targeted methyl mark (H3K27me3) was not affected (Fig. 3B and E).

Identification of a SMYD3 small-molecule inhibitor inducing CRC growth arrest

These results prompted us to perform a virtual screening by taking advantage of the three-dimensional structure of SMYD3 available in the Protein Data Bank with the aim of identifying new small-molecule inhibitors targeting its histone methyltransferase catalytic site. A structure-based high-throughput docking screening was performed in order to early identify novel lead compounds capable of inhibiting SMYD3 catalytic activity (Fig. 4A and B). By means of molecular docking techniques, we screened in silico the Asinex subset of CoCoCo databases as described in the methods section, and selected 15 molecules that were acquired and tested experimentally. After an initial screening performed using these molecules at a single concentration, we restricted our interest on Compound 5 (BCI-121). At 100 μM, this molecule caused a significant reduction in global tri-methylation and di-methylation levels of lysine 4 on histone H3 (Fig. 4C and D and Table S1). These data suggested that BCI-121 was the best candidate for SMYD3 inhibition within the initial set of compounds selected through the virtual screening procedure. To test whether BCI-121 was directly targeting SMYD3 enzymatic activity, we performed an in vitro methylation assay, using purified histones as a substrate. In agreement with previous reports (Van Aller et al., 2012; Mazur et al., 2014), SMYD3 preferentially methylated histone H4, and the presence of BCI-121 impaired SMYD3-mediated H4 in vitro methylation (Fig. 5A). Importantly, BCI-121 significantly reduced proliferation of HT29 (by 46%) and HCT116 (by 54%) cells at 72 h (Fig. 5B and C) and decreased the expression levels of SMYD3 target genes (Fig. 5D and E).

Cell response to BCI-121 treatment depends on SMYD3 expression levels

To further characterize the effects of BCI-121 treatment in CRC at the biological level, we extended our analysis to a CRC cell line panel. Interestingly, BCI-121 treatment only

affected proliferation of cancer cell lines expressing high levels of SMYD3 (Fig. 6A). Importantly, treatment with BCI-121 consistently replicated the biological features of genetic ablation in terms of targeted methyl marks reduction (Fig. 6B). This preliminary screening suggests that tumor cell types might be classified based on SMYD3 expression levels in order to efficiently design a SMYD3-targeted epigenetic cancer therapy. To confirm our hypothesis, we evaluated SMYD3 expression in cancer cell lines of different origin (lung, breast, prostate, ovarian cancer, and hepatocellular carcinoma) and found that only cell lines derived from tumors expressing high levels of SMYD3 protein proved responsive to BCI-121 treatment, as measured by inhibition of cell proliferation (Fig. 6C, D, and E). These data strongly support a therapeutic approach based on the use of the proposed BCI-121 compound as a new antitumor agent.

SMYD3 in ovarian cancer

To our knowledge, these results are the first evidence indicating that SMYD3 is involved in ovarian cancer. The high levels of SMYD3 expression detected in OVCAR-3 cells, along with the strong reduction in proliferation rate observed upon BCI-121 treatment, prompted us to better characterize the biological effect of SMYD3 inhibition in this type of cancer. To this purpose, we used OVCAR-3 and SKOV-3 ovarian cancer cell lines and found that SMYD3 genetic ablation decreased the global methylation levels of histone H3 and H4 (H3K4me2 and H4K5me), while a non-targeted methyl mark (H3K27me3) was not affected (Fig. 7A). Moreover, our data showed that SMYD3 is required for proper ovarian cancer cell growth as well as for the expression of its target genes (Fig. 7B and C). Indeed, SMYD3 genetic ablation significantly reduced proliferation of both SKOV-3 (by 35%) and OVCAR-3 (by 65%) cells.

SMYD3 regulates S/G2 transition in cancer cells

To get insight into SMYD3 function during proliferation, we performed a FACS analysis of CRC cells (HT29) treated or not with BCI-121 treated or not with BCI-121. Our data unveiled a considerable effect on cell cycle progression with a significant increase in S phase population. These results suggest that SMYD3 regulates the S/G2 transition (Fig. 8A). To better characterize the role of SMYD3 in the S/G2 phase transition, we performed a BrdU incorporation assay by synchronizing CRC cells. We used a synchronization model (O'Connor and Jackman, 1998) based on a double thymidine block causing cells to arrest in late G1 phase. With this protocol, cells enter into S phase 4 h after thymidine release and progress into G2/M phase 8 h after release (www.sbcellcycle.org; State-of-the-art in human cell synchronization; DIAMONDS Deliverable 1-D1.1.3). Synchronization by double thymidine block was performed during treatment with BCI-121 and/or DMSO. Our results indicate that cells treated with BCI-121 failed to exit S phase. Indeed, these cells displayed increased BrdU incorporation revealing S phase enrichment compared to untreated cells (Fig. 8B).

Molecular modeling and binding competition experiments in vitro and in cell lines

In order to get further insight into the mechanisms underlying SMYD3 inhibition by BCI-121, we performed surface plasmon resonance experiments to investigate the binding modes of this compound with molecular modelling techniques. The target protein SMYD3

was immobilized through an affinity capture method as a SMYD3-GST fusion protein to an anti-GST antibody covalently bound to a CM5 sensor chip. This oriented immobilization approach ensured that the histone binding site of SMYD3 was accessible for interaction. H4 histone binding to SMYD3 was analyzed at different analyte concentrations, and an affinity K_D of 1.18×10^{-5} M was determined based on the association and dissociation rate constants (k_{on} 357.7 ± 28.0 M^{-1} s^{-1}; k_{off} $4.23 \times 10^{-3} \pm 2.9 \times 10^{-5}$ s^{-1}; $K_D = k_{off}/k_{on}$). Then, compound BCI-121 was assessed as a potential inhibitor of SMYD3/histone binding. H4 histone was injected at 72.03 μM, alone or in the presence of BCI-121, in 1:1 and 1:2.5 [histone peptide]:[BCI-121] molar ratios. At these ratios, BCI-121 inhibited histone H4 binding by 36.5% and 51.0%, respectively (Fig. 9A), indicating that the mechanism foreseen by docking calculation can indeed occur through competition at the histone binding site. BCI-121 binds in the inner part of the lysine channel connecting the cofactor binding site to the histone peptide binding site. This substrate binding site is formed within the SET and post-SET domains and consists in a deep and narrow substrate binding pocket where the structure of BCI-121 is predicted to bind. A closer look at this binding mode suggests that the 4-carboxamide moiety of the piperidine ring is oriented toward the cofactor binding site and forms two hydrogen bonding interactions with Ser202. The carbamoyl group undergoes another hydrogen bonding between the nitrogen of the amide group and the backbone of Tyr239. All other interactions are basically formed with the hydrophobic residues that comprise the narrow binding pocket of the histone lysine residue, consistent with the hydrophobic nature of its alkylic side chain (Fig. 9B and Figure S1).Interestingly, the opening of the substrate binding pocket reveals several acidic residues, such as Glu192 and Asp241, which do not directly interact with BCI-121, suggesting that BCI-121 scaffold might be optimized to create additional interactions in order to improve potency (Figure S2). These results prompted us to test the ability of BCI-121 to affect histone binding to SMYD3 in cell line models. Hence, we analyzed SMYD3 occupancy at binding sites located in the promoters of its target genes in two different cancer cell lines (HCT116 and OVCAR-3) treated or not with BCI-121. Our data confirmed that BCI-121 competes with histones for binding to SMYD3 also in a cellular setting, as shown by its reduced binding to the promoter region of target genes (Fig. 9C). The functional readout of this activity is a significant reduction of target gene mRNA expression (Fig. 9D).

Dose-dependence of BCI-121 treatment

In order to find the lowest concentration affecting SMYD3 activity in cell cultures, we established a dose-dependent curve for BCI-121 (1, 10, 30, 60, 100 μM) and evaluated its anticancer activity in a CRC cell line (HT29) by measuring the cell proliferation index and by evaluating the global level of methylation at SMYD3-targeted (H4K5me and H3K4me2) and non-targeted (H3K27me3) sites. Our results show that there is a dose-dependent relationship between SMYD3 impairment and both inhibition of proliferation (Fig. 10A) and reduction of targeted methyl marks (H4K5me and H3K4me2) (Fig. 10B). A similar correlation was also observed with the level of MEK-ERK signaling activity (Fig. 10B). Consistent with previous results, the dose-dependent effect on cell growth was detected in cancer cells expressing high levels of SMYD3 (HCT116 cells), while BCI-121 treatment failed to inhibit proliferation in cancer cells with low levels of SMYD3 (LS174T cells) (Fig.

10C). Collectively, these data indicate that BCI-121 reproduces the effects of SMYD3-targeted RNAi.

Discussion

SMYD3 is a member of the SMYD subfamily of histone methyltransferases that is highly overexpressed in several types of cancer and has been suggested to play an oncogenic role, including stimulation of proliferation, adhesion, and migration. Here we showed that SMYD3 is significantly upregulated (both at the mRNA and protein level) throughout CRC tumorigenesis, as indicated by experiments on the $APC^{Min/+}$ mice preclinical model (+/− AOM). Of note, expression of SMYD3 target genes (cMET, TERT, WNT10B, CDK2) was upregulated as well, revealing a significant correlation with SMYD3 protein levels. In culture, we found that SMYD3 was overactivated in various cancer cell lines of different origin (colorectal, lung, pancreatic, and prostate cancer) and showed that these cells are highly sensitive to its genetic depletion. Moreover, our analysis revealed for the first time the involvement of SMYD3 in ovarian cancer cell growth. Based on these data, we speculated that the use of specific inhibitors might help to gain a better understanding of the role of SMYD3 in tumorigenesis and could also be the basis for future pharmacological interventions. Indeed, while other epigenetics drugs targeting EZH2, another component of the lysine(K)-methyltransferases (KMTs) family, are currently in clinical trials for the treatment of various human cancers, no SMYD3-specific compound has been identified so far. Thus, we envisioned to specifically target SMYD3 catalytic function by means of small-molecule inhibitors in order to preferentially target cancer cells. To this purpose, based on the crystallography structure of SMYD3, we took advantage of molecular design techniques to search for new small molecules that could inhibit its catalytic activity. Since no previous knowledge on specific SMYD3 inhibitors was available, our selection was based on the conformations of the substrate binding site and on the possibility to accommodate specific molecules. After testing several compounds, we identified a piperidine-4-carboxamide acetanilide compound (BCI-121) that was effective in cell lines at low micromolar concentrations and was able to impair SMYD3-mediated H4 methylation in vitro, showed antiproliferative properties in cancer cell lines overexpressing SMYD3 and, in general, replicated the effects of SMYD3-targeted RNAi. Indeed, cancer cells treated with BCI-121 showed a significant reduction in their growth ability and accumulated in the S phase of the cell cycle, suggesting that SMYD3 might be required for proper cell cycle progression through the S/G2 boundary. Efficacy of the selected compound was also demonstrated with histone competition experiments through SPR techniques. Analysis of the molecular interactions of BCI-121 in the histone binding site suggests that its chemical structure may be optimized in order to improve potency, an approach that is expected to have important implications for the design of compounds amenable to therapeutic use.

Moreover, experiments performed in cancer cells showed that BCI-121 prevents SMYD3 recruitment on the promoters of its target genes and this event was correlated with reduced gene expression. Overall, the results presented here hold the basis for the development of new classes of SMYD3 inhibitors for therapeutic use in different cancer types. Importantly, it has been demonstrated that complete loss of SMYD3 function does not lead to a visible phenotype in mouse models, suggesting that the use of small molecules capable of impairing

SMYD3 activity as new anticancer agents might be associated with reduced side effects compared with other chemotherapeutics.

Conclusions

The US FDA recently approved three new epigenetic drugs for the treatment of specific human cancers, and small-molecule inhibitors targeting the KMT family component EZH2 are currently in clinical trials. However, despite the emerging pathophysiological role of SMYD3 in human cancer and its potential as a therapeutic target, no SMYD3 inhibitors have been identified so far (Helin and Dhanak, 2013). A better understanding of the role of SMYD3 in tumorigenesis might prove useful for the design of future pharmacological interventions. Indeed, a SMYD3-based therapeutic approach capable of inducing a cytostatic effect on different types of tumor cells could be a valuable tool in cancer treatment. The ability of BCI-121 to arrest cancer cells at the S/G2 boundary of the cell cycle suggests that this small molecule could improve the effects of conventional chemotherapy by acting on the DNA damage checkpoints, and it can be hypothesized that BCI-121 could also sensitize cancer cells to S/G2 phase-specific chemotherapeutic agents. Our study provides an important advancement in this research area, since it describes for the first time a non-peptide inhibitor of SMYD3. Indeed, these data represent the proof of principle that SMYD3 can be pharmacologically modulated by means of small-molecule inhibitors. We believe that these results may have a strong impact on the identification of new molecules amenable to use as novel therapeutic agents.

Supporting Information

Refer to Web version on PubMed Central for supplementary material.

Acknowledgments

We thank Dr. Francesco Paolo Jori for his helpful discussion during the preparation of the manuscript and editorial assistance. A.P. is supported by an Italian Foundation for Cancer Research (FIRC) fellowship, C.B. and E.F. are supported by Alma Mater Studiorum – University of Bologna (Italy).

Contract grant sponsor: Emilia Romagna Start-Up grant of the Associazione Italiana per la Ricerca sul Cancro (AIRC);

Contract grant number: 6266.

Contract grant sponsor: Associazione Italiana per la Ricerca sul Cancro;

Contract grant number: AIRC_MFAG 5386.

Contract grant sponsor: International Association for Cancer Research;

Contract grant number: AICR 14-0149.

Contract grant sponsor: Associazione Italiana per la Ricerca sul Cancro (AIRC);

Contract grant number: IG10177.

Contract grant sponsor: FIRB – FUTURO IN RICERCA from the Italian MIUR;

Contract grant number: RBFR12VP3Q_003.

References

Biggar KK, Li SSC. Non-histone protein methylation as a regulator of cellular signalling and function. Nat Rev Mol Cell Biol. 2015; 16:5–17. [PubMed: 25491103]

Chi P, Allis CD, Wang GG. Covalent histone modifications-miswritten, misinterpreted, and mis-erased in human cancers. Nat Rev Cancer. 2010; 10:457–469. [PubMed: 20574448]

Chiacchiera F, Matrone A, Ferrari E, Ingravallo G, Lo Sasso, Petruzzelli S, Salvatore M, Moschetta L, Simone A. P38alpha blockade inhibits colorectal cancer growth in vivo by inducing a switch from HIF1alpha- to FoxO-dependent transcription. Cell Death Differ. 2009; 16:1203–1214. [PubMed: 19343039]

Cock-Rada AM, Medjkane S, Janski N, Yousfi N, Perichon M, Chaussepied M, Chluba J, Langsley G, Weitzman JB. SMYD3 promotes cancer invasion by epigenetic upregulation of the metalloproteinase MMP-9. Cancer Res. 2012; 72:810–820. [PubMed: 22194464]

Copeland RA, Solomon ME, Richon VM. Protein methyltransferases as a target class for drug discovery. Nat Rev Drug Discov. 2009; 8:724–732. [PubMed: 19721445]

De Robertis M, Massi E, Poeta ML, Morini S, Cecchetelli L, Signori E, Fazio VM. The AOM/DSS murine model for the study of colon carcinogenesis: From pathways to diagnosis and therapy studies. J Carcinog. 2011; 24:10–19.

Del Rio A, Barbosa AJM, Caporuscio F, Mangiatordi GF. CoCoCo: A free suite of multiconformational chemical databases for high-throughput virtual screening purposes. Mol Biosyst. 2010; 6:2122–2128. [PubMed: 20694263]

Foreman KW, Brown M, Park F, Emtage S, Harriss J, Das C, Zhu L, Crew A, Arnold L, Shaaban S, Tucker P. Structural and functional profiling of the human histone methyltransferase SMYD3. PLoS One. 2011; 6:e22290. [PubMed: 21779408]

Gaedcke J, Grade M, Jung K, Camps J, Jo P, Emons G, Gehoff A, Sax U, Schirmer M, Becker H, Beissbarth T, et al. Mutated KRAS results in overexpression of DUSP4, a MAP-kinase phosphatase, and SMYD3, a histone methyltransferase, in rectal carcinomas. Genes Chromosomes Cancer. 2010; 49:1024–1034. [PubMed: 20725992]

Greer EL, Shi Y. Histone methylation: A dynamic mark in health, disease, and inheritance. Nat Rev Genet. 2012; 13:343–357. [PubMed: 22473383]

Guil S, Soler M, Portela A, Carrère J, Fonalleras E, Gómez A, Villanueva A, Esteller M. Intronic RNAs mediate EZH2 regulation of epigenetic targets. Nat Struct Mol Biol. 2012; 19:664–670. [PubMed: 22659877]

Hamamoto R, Furukawa Y, Morita M, Iimura Y, Silva FP, Li M, Yagyu R, Nakamura Y. SMYD3 encodes a histone methyltransferase involved in the proliferation of cancer cells. Nat Cell Biol. 2004; 6:731–740. [PubMed: 15235609]

Hamamoto R, Silva FP, Tsuge M, Nishidate T, Katagiri T, Nakamura Y, Furukawa Y. Enhanced SMYD3 expression is essential for the growth of breast cancer cells. Cancer Sci. 2006; 97:113–118. [PubMed: 16441421]

Helin K, Dhanak D. Chromatin proteins and modifications as drug targets. Nature. 2013; 502:480–488. [PubMed: 24153301]

Klein AM, Zaganjor E, Cobb MH. Chromatin-tethered MAPKs. Curr Opin Cell Biol. 2013; 25:272–277. [PubMed: 23434067]

Kim H, Heo K, An W. Requirement of histone methyltransferase SMYD3 for estrogen receptor-mediated transcription. J Biol Chem. 2009; 284:19867–19877. [PubMed: 19509295]

Kunizaki M, Hamamoto R, Silva FP, Yamaguchi K, Nagayasu T, Shibuya M, Nakamura Y, Furukawa Y. The lysine 831 of vascular endothelial growth factor receptor 1 is a novel target of methylation by SMYD3. Cancer Res. 2007; 67:10759–10765. [PubMed: 18006819]

Liu C, Fang X, Ge Z, Jalink M, Kyo S, Björkholm M, Gruber A, Sjöberg J, Xu D. The telomerase reverse transcriptase (hTERT) gene is a direct target of the histone methyltransferase SMYD3. Cancer Res. 2007; 67:2626–2631. [PubMed: 17363582]

Liu Y, Luo X, Deng J, Pan Y, Zhang L, Liang H. SMYD3 overexpression was a risk factor in the biological behavior and prognosis of gastric carcinoma. Tumour Biol. 2014; doi: 10.1007/s13277-014-2891-z

Luo XG, Zhang CL, Zhao WW, Liu ZP, Liu L, Mu A, Guo S, Wang N, Zhou H, Zhang TC. Histone methyltransferase SMYD3 promotes MRTF-A-mediated transactivation of MYL9 and migration of MCF-7 breast cancer cells. Cancer Lett. 2014; 344:129–137. [PubMed: 24189459]

Mazur PK, Reynoird N, Khatri P, Jansen PWTC, Wilkinson AW, Liu S, Barbash O, Van Aller GS, Huddleston M, Dhanak D, Tummino PJ, et al. SMYD3 links lysine methylation of MAP3K2 to Ras-driven cancer. Nature. 2014; 510:283–287. [PubMed: 24847881]

O'Connor, PM.; Jackman, J. Synchronization of mammalian cells. Cell biology: A Laboratory Handbook. Celis, JE., editor. San Diego: Academic Press; 1998. p. 63-74.

Suganuma T, Workman JL. MAP kinases and histone modification. J Mol Cell Biol. 2012; 4:348–350. [PubMed: 22831833]

Tsuge M, Hamamoto R, Silva FP, Ohnishi Y, Chayama K, Kamatani N, Furukawa Y, Nakamura Y. A variable number of tandem repeats polymorphism in an E2F-1 binding element in the 5' flanking region of SMYD3 is a risk factor for human cancers. Nat Genet. 2005; 37:1104–1107. [PubMed: 16155568]

Van Aller GS, Reynoird N, Barbash O, Huddleston M, Liu S, Zmoos A, Sinnamon R, Le B Mas, Sage R, Garcia J, Tummino BA, et al. SMYD3 regulates cancer cell phenotypes and catalyzes histone H4 lysine 5 methylation. Epigenetics. 2012; 7:340–343. [PubMed: 22419068]

Varier RA, Timmers HTM. Histone lysine methylation and demethylation pathways in cancer. Biochim Biophys Acta. 2011; 1815:75–89. [PubMed: 20951770]

Zou JN, Wang SZ, Yang JS, Luo XG, Xie JH, Xi T. Knockdown of SMYD3 by RNA interference down-regulates c-Met expression and inhibits cells migration and invasion induced by HGF. Cancer Lett. 2009; 280:78–85. [PubMed: 19321255]

Europe PMC Funders Author Manuscripts

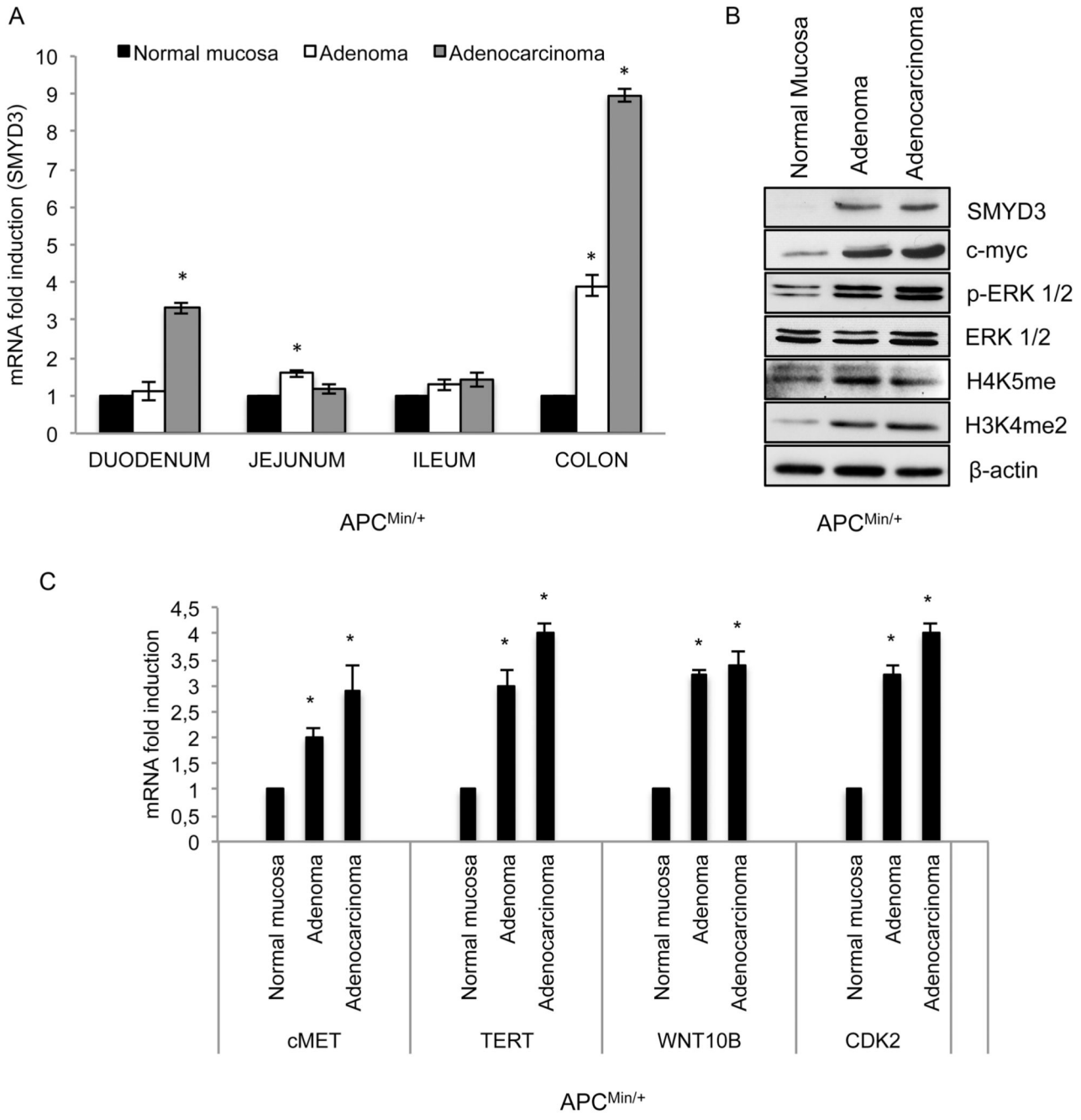

Fig. 1.

SMYD3 is upregulated during colorectal tumorigenesis (A) SMYD3 mRNA expression increases during transition from normal to tumor colon mucosa in $APC^{Min/+}$ mice. Tissue samples were obtained from control $APC^{Min/+}$ mice (n = 10) and $APC^{Min/+}$ mice treated with 12 mg/kg of azoxymethane (AOM) (n = 10). (B) Colorectal adenomas and carcinomas of $APC^{Min/+}$ mice overexpress SMYD3 protein and show increased global levels of H4K5me and H3K4me2. cMYC and pERK expression was assessed as an internal control of the experiment. (C) SMYD3 expression profile correlates with mRNA expression of its

Europe PMC Funders Author Manuscripts

target genes. β-actin was used as a loading control for immunoblotting and for real-time PCR data normalization. Statistical analysis was performed using Student's *t*-tail test; $*P < 0.05$ was considered statistically significant.

Europe PMC Funders Author Manuscripts

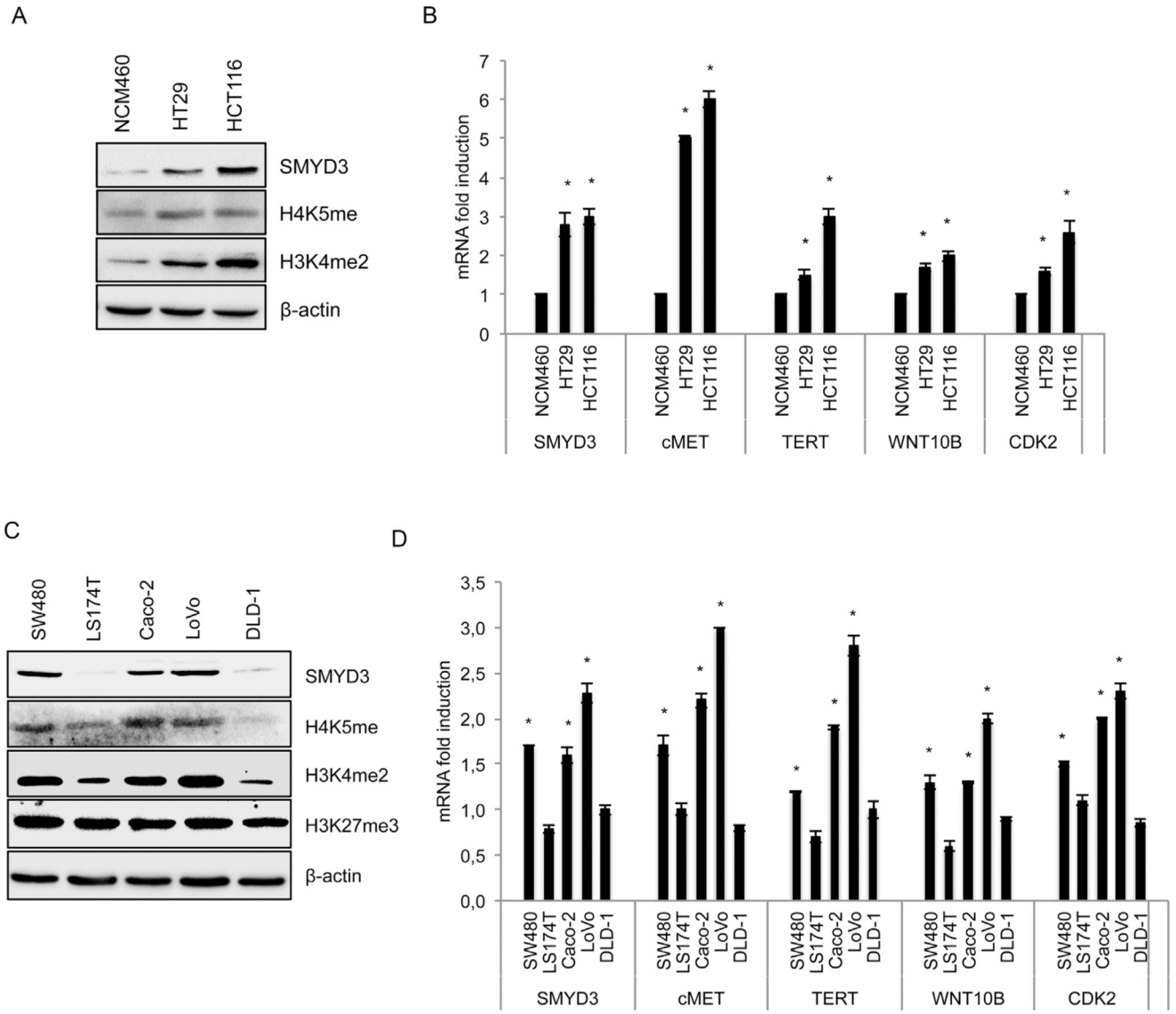

Fig. 2.

SMYD3 shows high levels of expression in CRC cell lines. SMYD3 protein (A, C) and mRNA (B, D) expression is enhanced in several human CRC cell lines. (A, C) SMYD3 protein expression correlates with the global level of targeted histone methyl marks [H3K4me2 and H4K5me] and (B, D) with the transcriptional activation of its target genes in the indicated cell lines. The levels of a SMYD3 non-targeted methyl mark [H3K27me3] are not modulated. In B and D, fold induction is normalized to mRNA levels observed in NCM460 cells (arbitrarily set as 1). β-actin was used as a loading control for immunoblotting and for real-time PCR data normalization. Statistical analysis was performed using Student's *t*-tail test; $*P < 0.05$ was considered statistically significant.

Europe PMC Funders Author Manuscripts

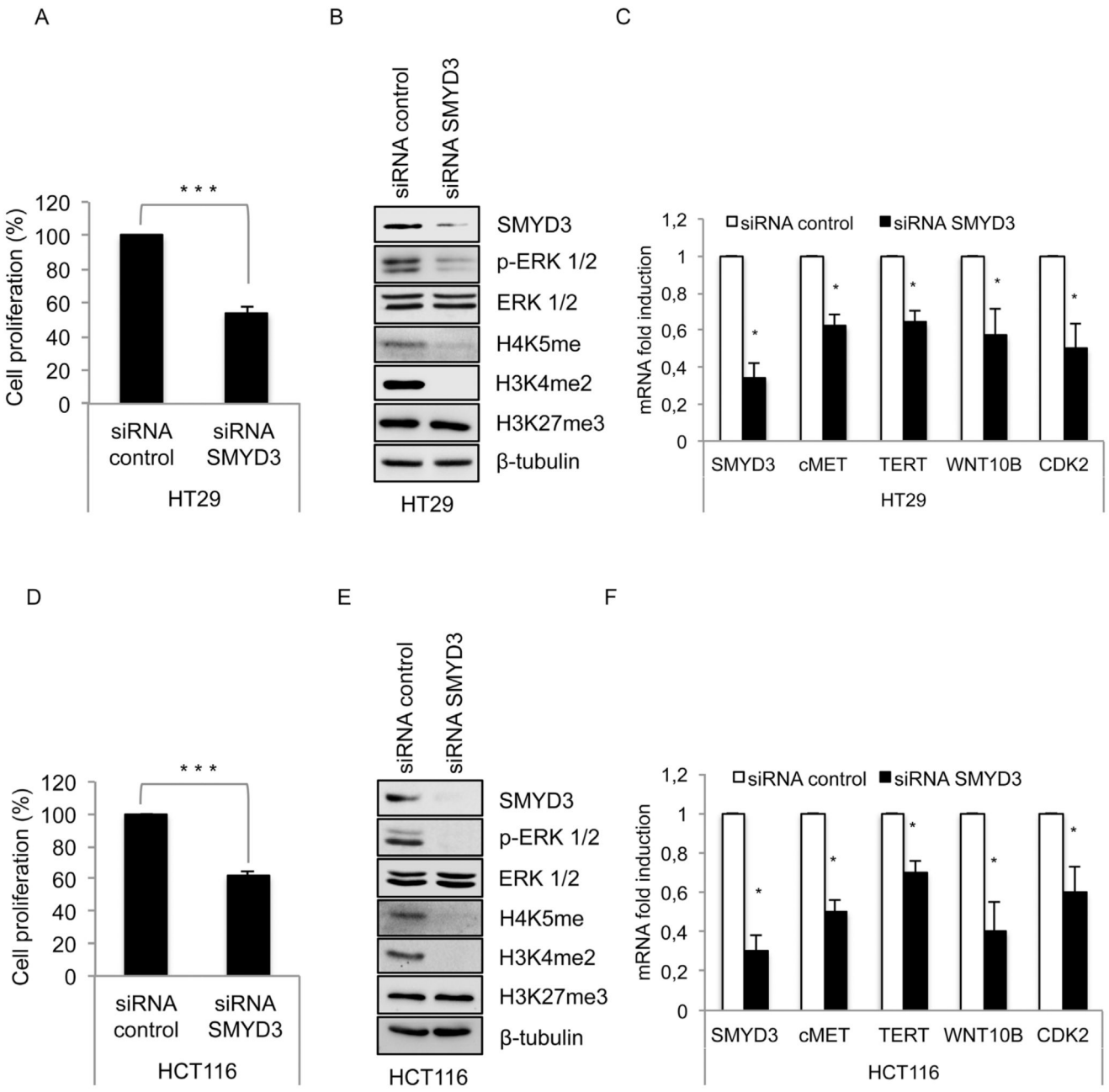

Fig. 3.

SMYD3 is required for proper cancer cell growth. In HT29 (A, B, C) and HCT116 (D, E, F) CRC cell lines, SMYD3 inhibition by RNAi impairs cell proliferation (A, D), decreases the level of targeted histone methyl marks [H4K5me, H3K4me2] and ERK 1/2 activation (B, E), and reduces the expression level of SMYD3 target genes (C, F). A non-targeted methyl mark [H3K27me3] was not affected by RNAi-mediated SMYD3 ablation. HT29 and HCT116 CRC cell lines were transfected with control siRNAs or SMYD3-specific siRNAs for 48 h. Cell proliferation was calculated using the WST-1 assay. β-tubulin was used as a loading control for immunoblotting and β-actin was used for real-time PCR data normalization.

Statistical analysis was performed using Student's *t*-tail test; $*P < 0.05$, $**P < 0.01$, and $***P < 0.001$ were considered statistically significant.

Europe PMC Funders Author Manuscripts

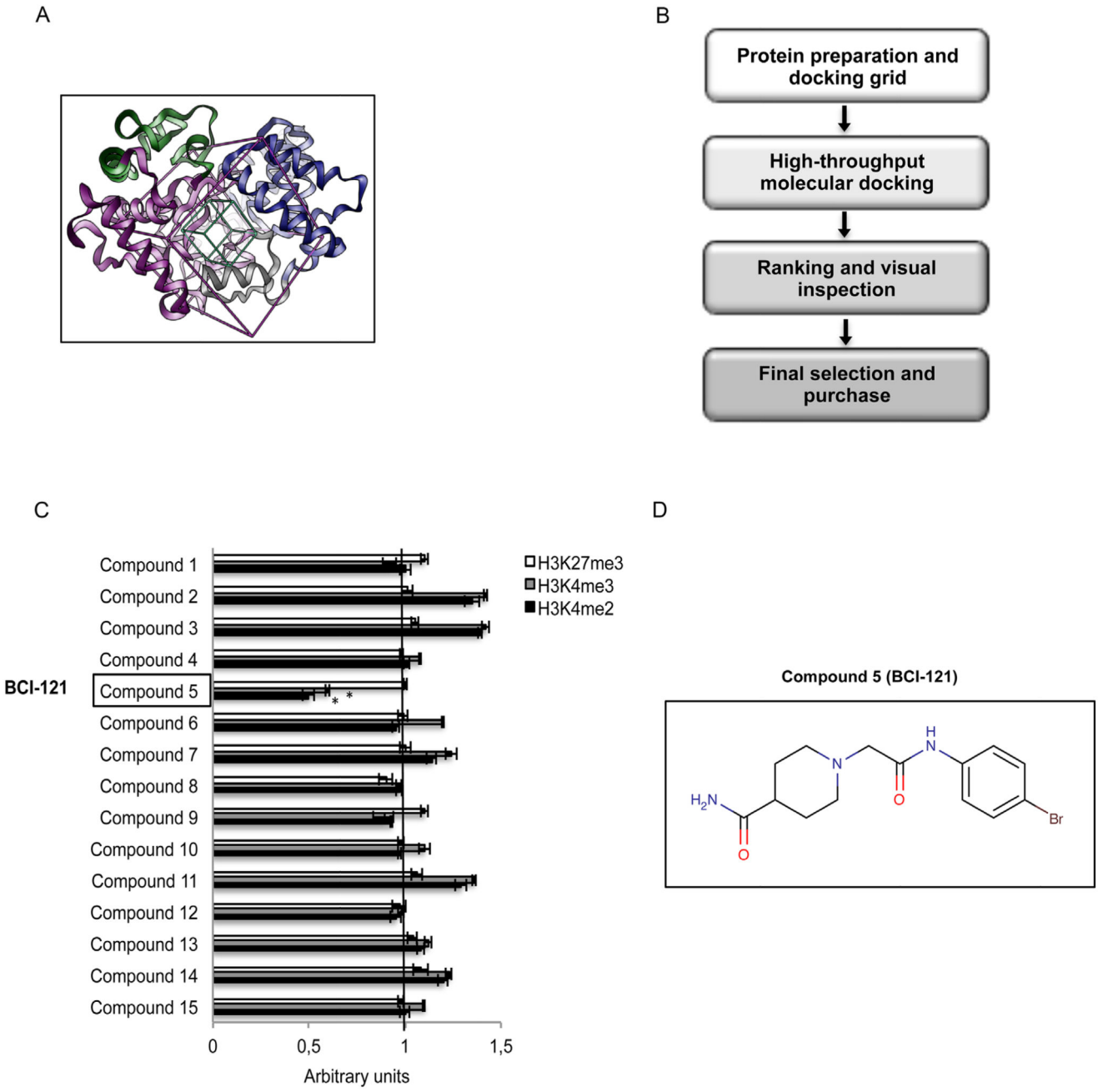

Fig. 4.

Virtual screening procedure allowing identification of BCI-121 as a promising candidate for SMYD3 inhibition. (A) Structure of full-length SMYD3 highlighting the N-terminal SET domain (purple), the MYND domain (yellow), the post-SET domain (gray), and the C-terminal region (blue). The boxes define the area of the protein - centered on the histone binding site - that was considered to perform the docking screening calculation. The green box identifies the area containing at least one atom of the putative ligand, while the purple box identifies the area where all atoms of the ligands should lie. (B) Schematic representation of the virtual screening procedure. (C) Compound 5 [BCI-121] is the best

candidate small molecule for SMYD3 inhibition among the initial set of 15 compounds selected through the virtual screening procedure. The global level of SMYD3 targeted [H3K4me2 and H3K4me3] and non-targeted [H3K27me3] histone methyl marks was measured by immunoblot in nuclear enriched fractions of CRC cells (HT29) treated with each compound (100 μM). Values shown correspond to histone methyl mark levels quantified by densitometric analysis and normalized to the loading control Lamin A/C (arbitrary units, untreated control at 48h = 1). (D) Structural formula of the selected compound BCI-121 (Figure generated with MarvinSketch v6.0.0 http://www.chemaxon.com). Statistical analysis was performed using Student's *t*-tail test; $*P < 0.05$ was considered statistically significant.

Europe PMC Funders Author Manuscripts

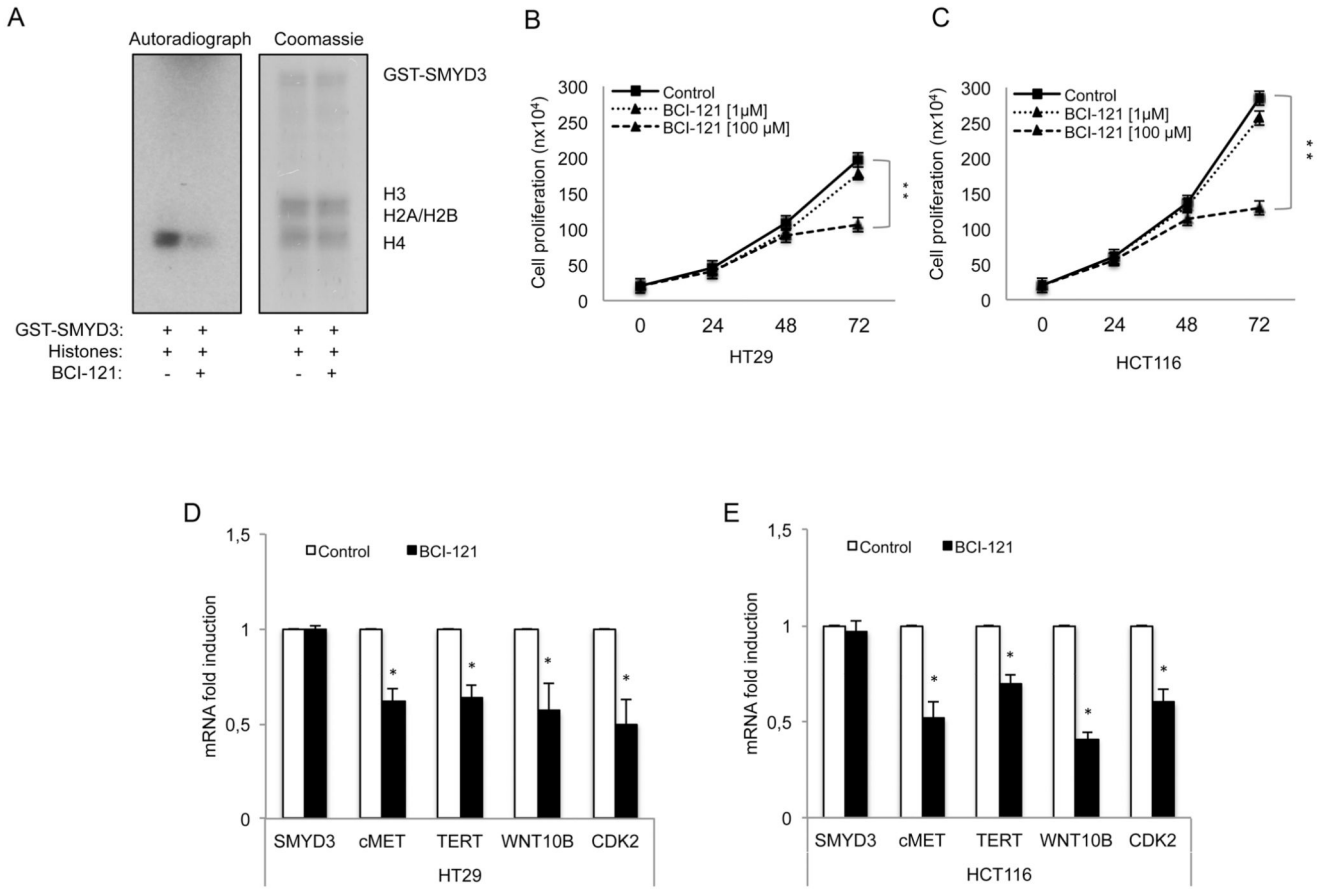

Fig. 5.

BCI-121 inhibits SMYD3 activity in vitro and in CRC cell models and affects cell proliferation. (A) In vitro methylation assay using the indicated recombinant SMYD3 protein on a mixture of calf thymus histones in the presence and/or absence of BCI-121 showing a significant decrease in H4 methylation. Autoradiograph and Coomassie stained (loading control) gels are shown. BCI-121 inhibits cell proliferation in HT29 (B) and HCT116 (C) cells in a dose- and time-dependent manner. Cell proliferation was assessed by cell counting. The data presented are the mean values obtained for each analyzed time point (n = 4). (D, E) BCI-121 100 μM decreases the expression levels of SMYD3 target genes in both cell lines (the 48 h time point was evaluated). β-actin was used for normalization of real-time PCR data. Statistical analysis was performed using Student's *t*-tail test; $*P < 0.05$, $**P < 0.01$, and $***P < 0.001$ were considered statistically significant.

Europe PMC Funders Author Manuscripts

Europe PMC Funders Author Manuscripts

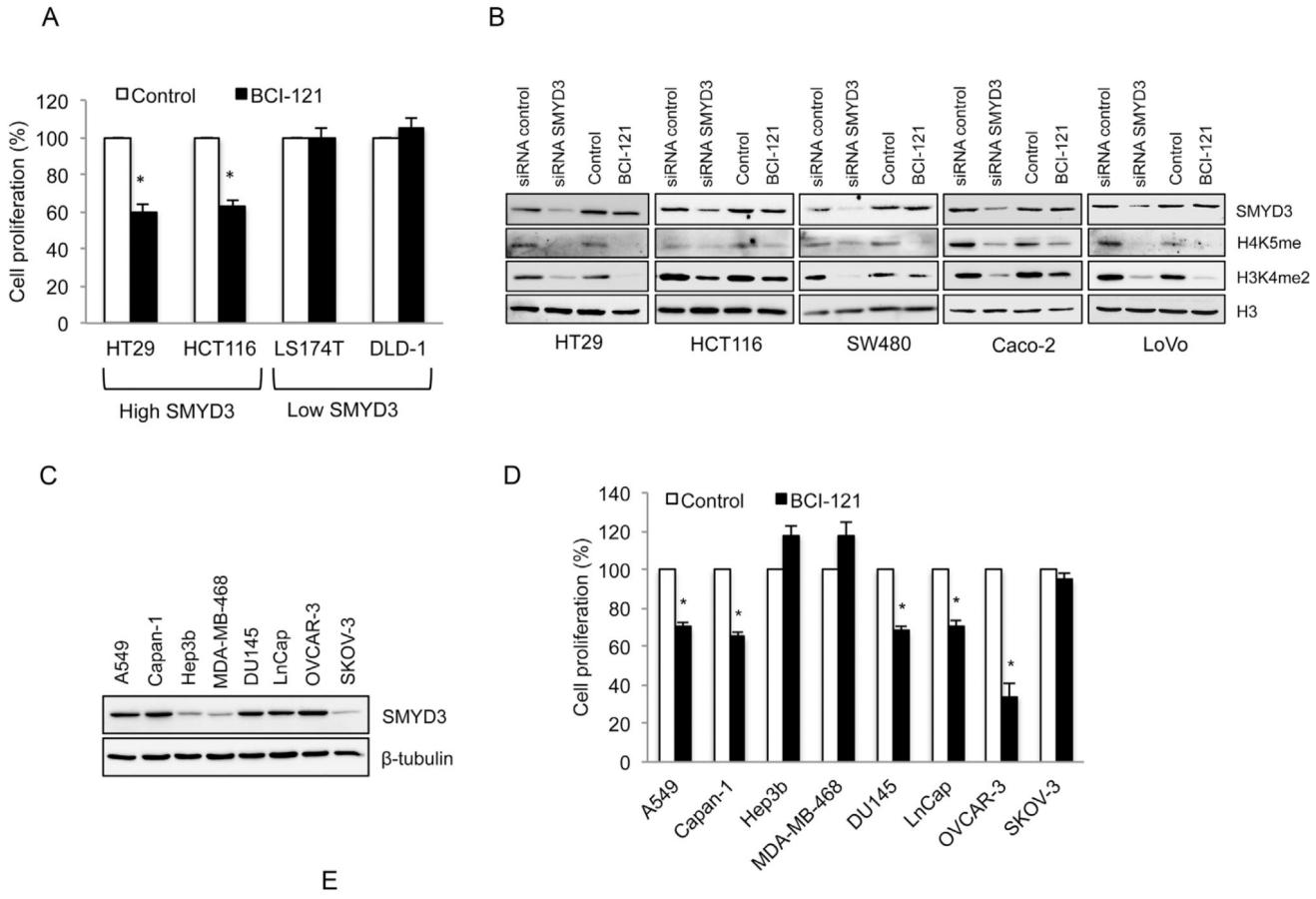

E

SMYD3 expression level	Cancer type	Cell line	BCI-121 responsiveness
HIGH	CRC	HT29	+
		HCT116	+
		SW480	+
		Caco-2	+
		Lovo	+
	LC	A549	+
	PC	Capan-1	+
	PCa	DU145	+
		LnCap	+
	OC	OVCAR-3	+
LOW	CRC	LS174T	-
		DLD-1	-
	HCC	Hep3b	-
	BC	MDA-MB-468	-
	OC	SKOV-3	-

Fig. 6.

Basal SMYD3 expression levels predict BCI-121 treatment response. (A) Administration of BCI-121 affects proliferation of CRC cell lines expressing high levels of SMYD3. (B) BCI-121 treatment reduces targeted histone methyl marks [H4K5me and H3K4me2] to an extent comparable to that observed with RNAi. CRC cells were treated with BCI-121 and/or SMYD3-specific siRNAs for 48 h and H4K5me and H3K4me2 global levels were evaluated by immunoblot. H3 was used as a loading control. (C) SMYD3 protein is highly expressed in several cell lines derived from different types of cancer (A549 = lung cancer; Capan-1 =

pancreatic cancer; Hep3b = hepatocellular carcinoma; MDA-MB-468 = breast cancer; DU145 and LnCap = prostate cancer; OVCAR-3 and SKOV-3 = ovarian cancer). β-tubulin was used as a loading control. (D) BCI-121 treatment impaired proliferation of cancer cells with high expression levels of SMYD3, while cancer cells expressing low levels of SMYD3 were not affected. (E) SMYD3 protein levels in cell lines that proved responsive to BCI-121 treatment. Table summarizing the data obtained in the cell lines derived from the different types of cancer tested in this study [CRC, colorectal cancer; LC, lung cancer; PC pancreatic cancer; PCa, prostate cancer; OC, ovarian cancer; BC, breast cancer; HCC, hepatocellular carcinoma]. Cancer cell lines were treated with BCI-121 (100 μM) for 72 h (A) and 96 h (D) and cell proliferation was calculated using the WST-1 assay. Statistical analysis was performed using Student's *t*-tail test; $*P < 0.05$ was considered statistically significant.

Europe PMC Funders Author Manuscripts

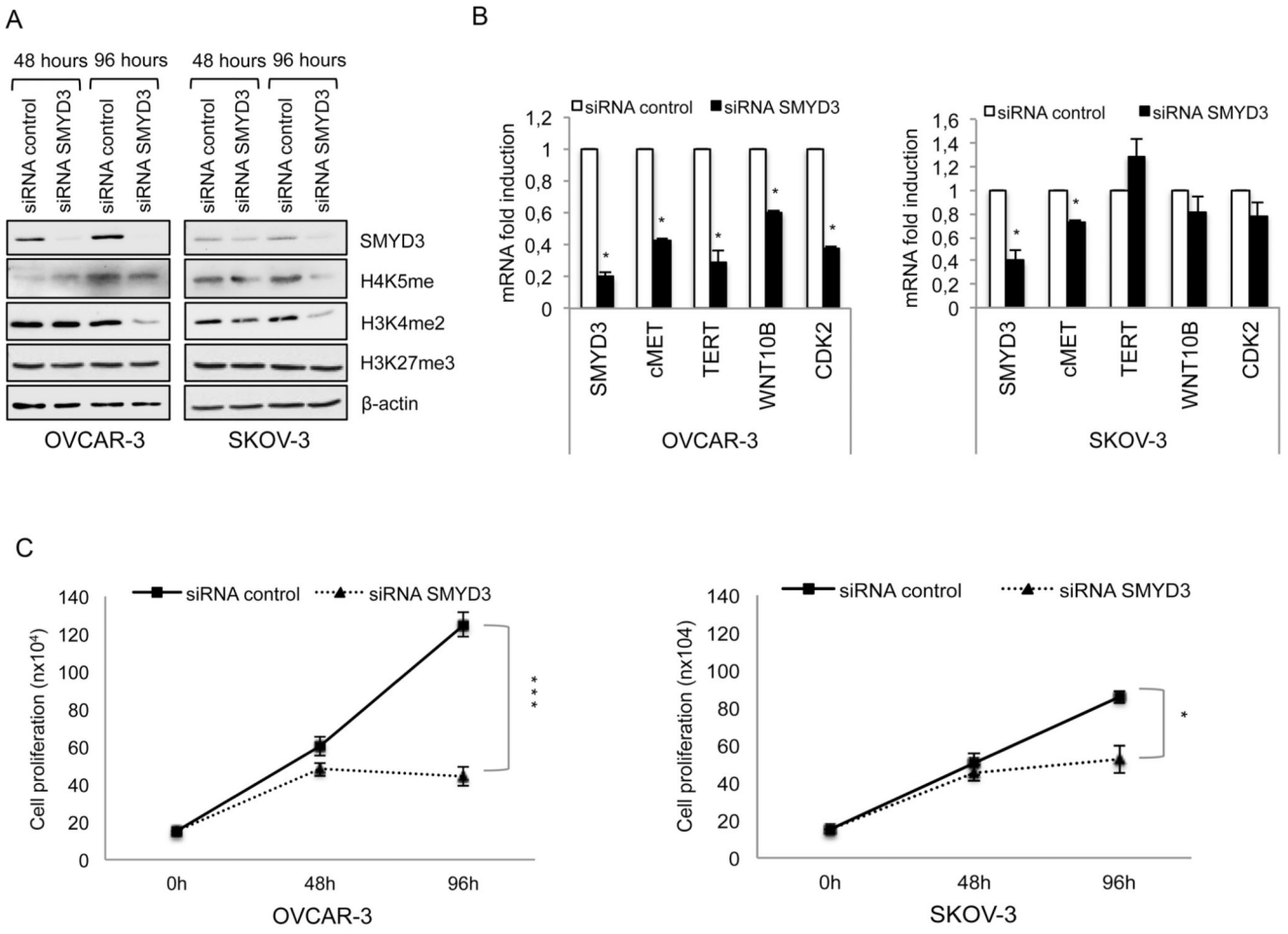

Fig. 7.

SMYD3 is required for proper ovarian cancer cell growth. (A) SMYD3 genetic ablation in ovarian cancer cell models decreases the global level of targeted histone methyl marks [H3K4me2 and H4K5me] without affecting a non-targeted methyl mark [H3K27me3]. (B) SMYD3 genetic ablation levels correlate with deregulated mRNA expression of its target genes and (C) with decreased cell proliferation rate. OVCAR-3 and SKOV-3 cells were transfected with control or SMYD3-specific siRNAs for 48 h and 96 h. Levels of methyl marks were determined by immunoblot; expression of target genes was analyzed by real-time PCR (the 48 h time point was evaluated). Cell proliferation was assessed by cell counting. The number of cells for each indicated time point is plotted. β-actin was used as a loading control for immunoblotting and for normalization of real-time PCR data. Statistical analysis was performed using Student's *t*-tail test; $*P < 0.05$, $**P < 0.01$, and $***P < 0.001$ were considered statistically significant.

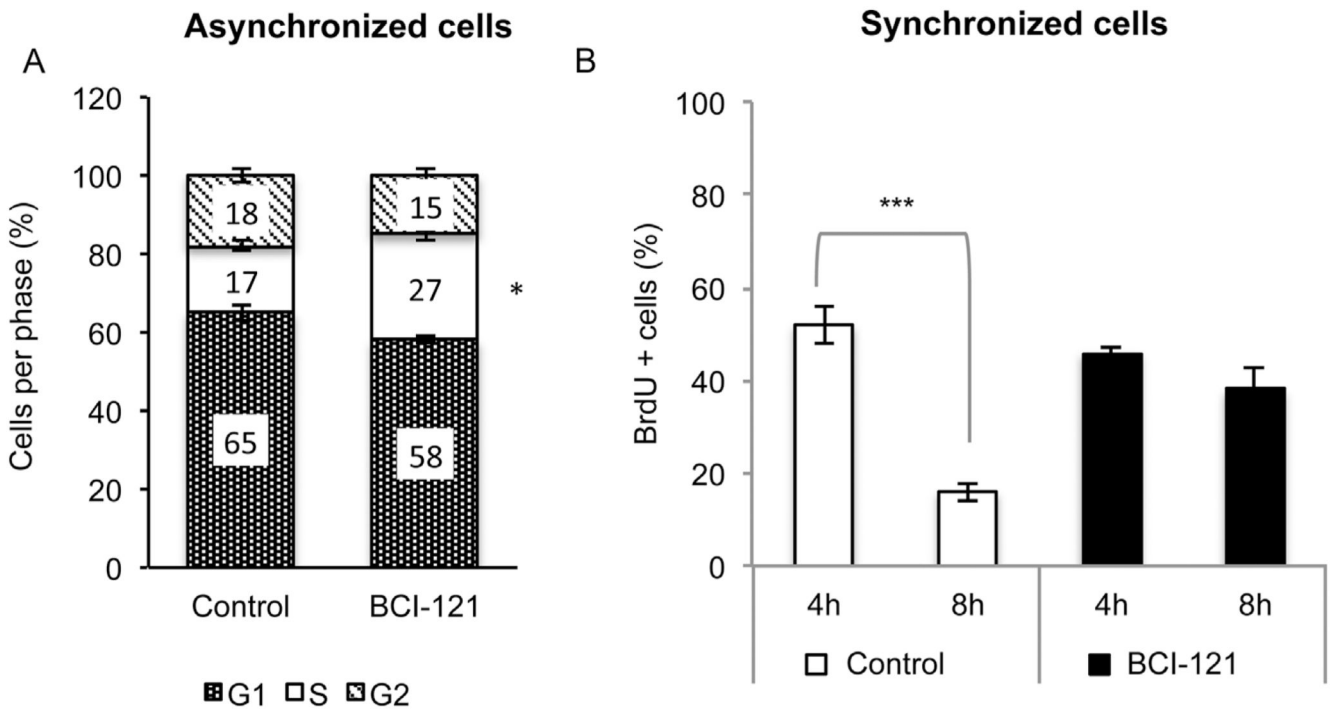

Fig. 8.

SMYD3 regulates S/G2 transition in cancer cells. (A) SMYD3 inhibition affects cell cycle progression in HT29 cells with a significant increase in the S-phase fraction. HT29 cells were treated with BCI-121 [100 μM] for 48 h and FACS analysis was performed following propidium iodide staining. (B) HCT116 synchronized cells treated with BCI-121 failed to exit S phase. Synchronization by double thymidine block was performed during treatment with BCI-121 (48 h). The 4 h (expected phase = S) and 8 h (expected phase = G2) post-release time points were analyzed through a BrdU incorporation assay to quantify BrdU-positive cells. Statistical analysis was performed using Student's *t*-tail test; $*P < 0.05$, $**P < 0.01$, and $***P < 0.001$ were considered statistically significant.

Europe PMC Funders Author Manuscripts

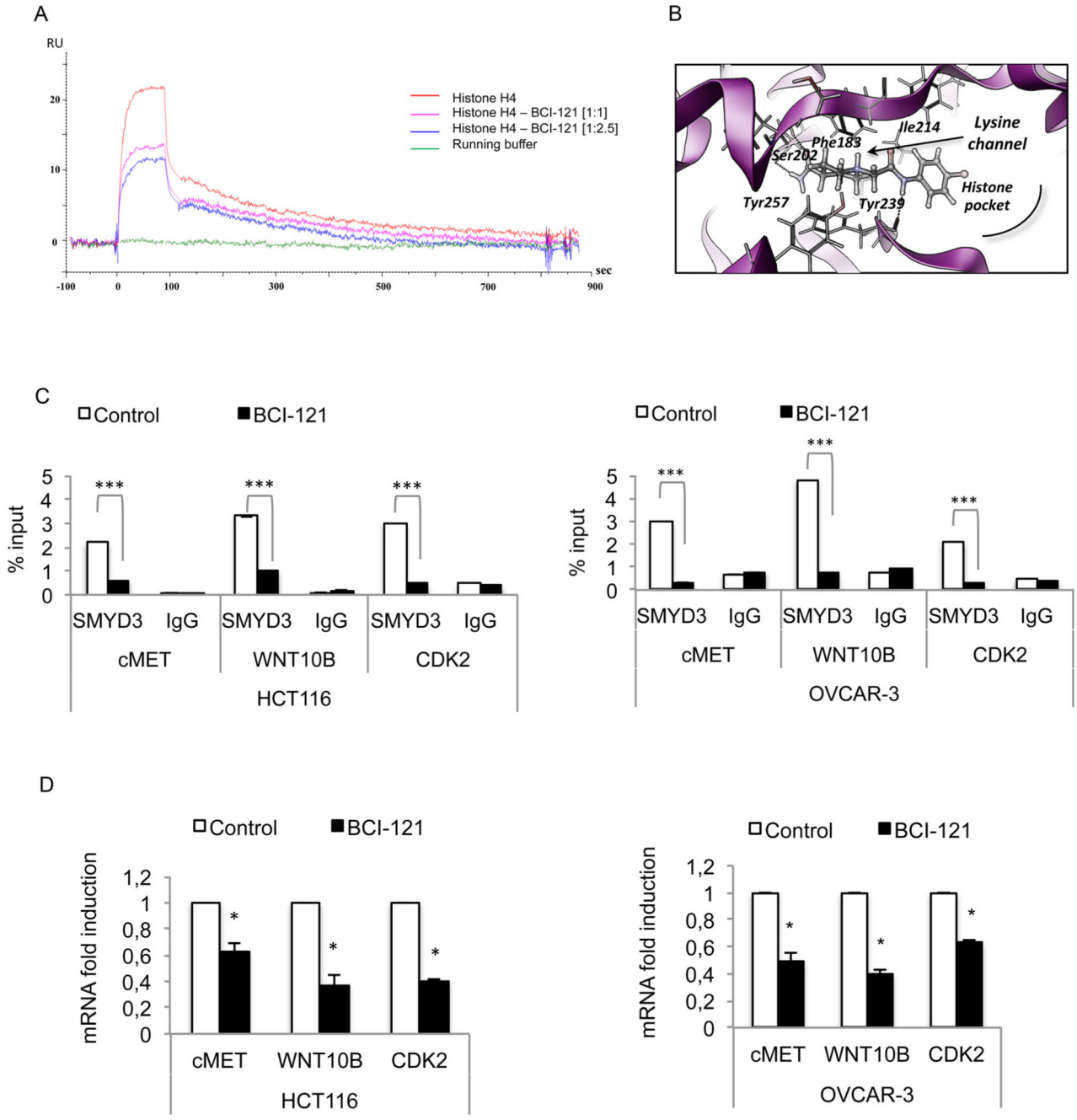

Fig. 9.

BCI-121 competes with target histones for SMYD3 binding in vitro and in cell line models. (A) Sensorgrams of H4 histone binding to SMYD3 in the presence and in the absence of BCI-121. (B) Predicted binding mode of BCI-121 to the histone binding site. (C) SMYD3 binding to the promoter of its target genes is abolished by the presence of BCI-121 in cancer cells. ChIP was performed in HCT116 and OVCAR-3 cells treated or not with BCI-121 (100 μM) for 72 h. Cells were cross-linked and immunoprecipitated with anti-SMYD3 and anti-IgG antibodies. The precipitated DNA was subjected to real-time PCR with specific primers,

which amplify SMYD3 binding site elements of human target gene promoters (cMET, WNT10B, and CDK2). IgGs were used as an immunoprecipitation control. (D) Transcriptional activation of target genes correlates with impaired binding of SMYD3. β-actin was used for real-time PCR data normalization. Statistical analysis was performed using Student's *t*-tail test; $*P < 0.05$ was considered statistically significant.

Europe PMC Funders Author Manuscripts

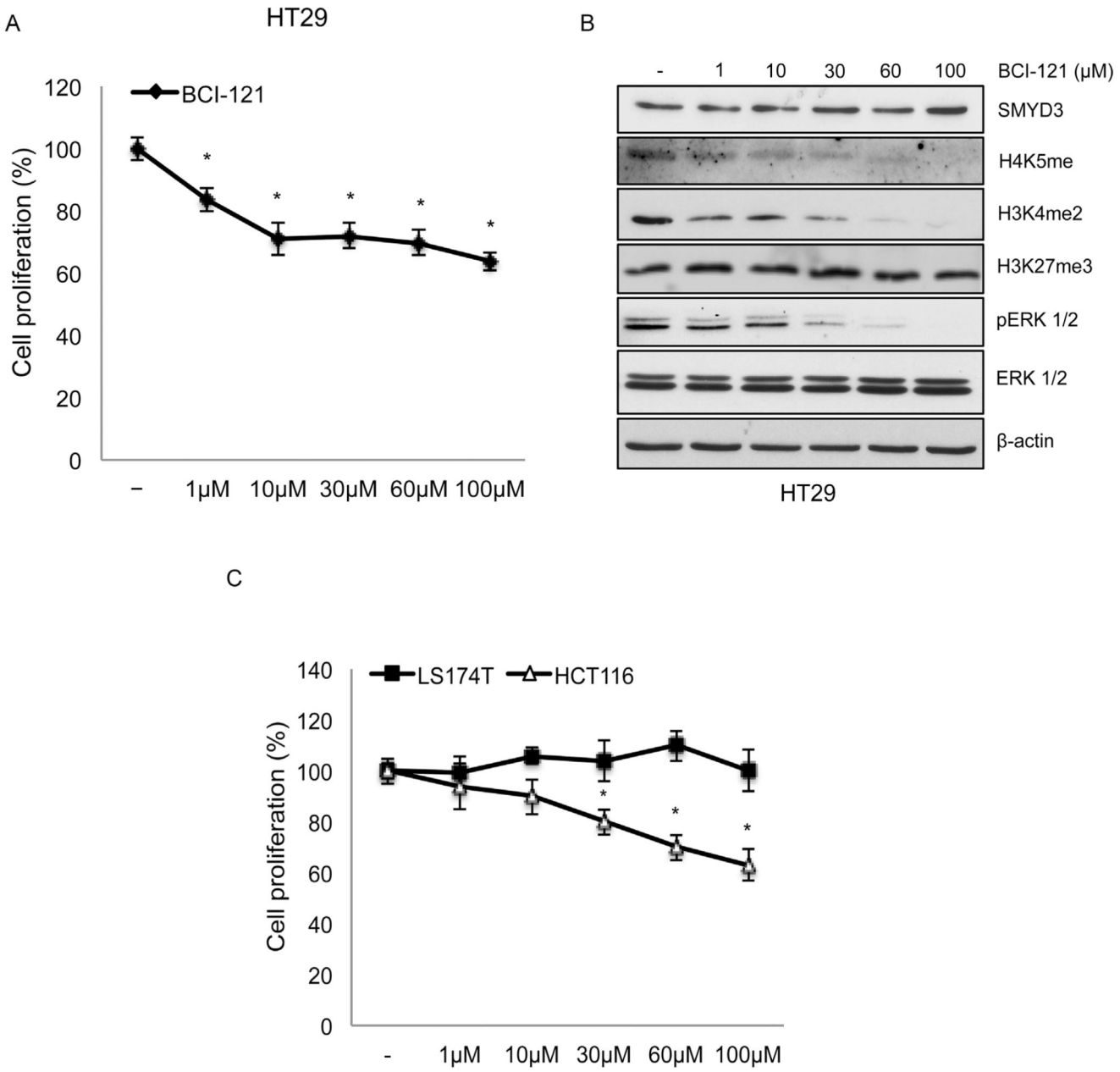

Fig. 10.

Dose-dependence of BCI-121 treatment in CRC cell lines. (A) BCI-121 treatment for 48 h induces a concentration-dependent reduction of CRC cell proliferation and (B) decreases the global levels of targeted histone methyl marks [H4K5me, H3K4me2] and ERK 1/2 activation. A non-targeted methyl mark [H3K27me3] was not affected. β-actin was used as a loading control for immunoblotting. (C) The dose-dependent effect of BCI-121 treatment (72 h) on cell growth is observed in cells expressing high levels of SMYD3 (HCT116), but not in cells with low levels of SMYD3 (LS174T). Cell proliferation was calculated using the

WST-1 assay. Statistical analysis was performed using Student's *t*-tail test; $*P < 0.05$, $**P < 0.01$, and $***P < 0.001$ were considered statistically significant.

Europe PMC Funders Author Manuscripts